Molecular insertion regulates the donor-acceptor interactions in cocrystals for the design of piezochromic luminescent materials

Chunguang Zhai
Jilin University https://orcid.org/0000-0002-6707-0359
Xiu Yin
Jilin University
Shifeng Niu
Jilin University
Mingguang Yao (yaomg@jlu.edu.cn)
Jilin University
Shuhe Hu
Jilin University
Jiajun Dong
Jilin University
Yuchen Shang
Jilin University
Zhigang Wang
Jilin University https://orcid.org/0000-0002-3028-5196
Quanjun Li
Jilin University https://orcid.org/0000-0002-4718-4156
Bertil Sundqvist
Jilin University
Bingbing Liu
Jilin University https://orcid.org/0000-0003-3989-0891

Article

Keywords: piezochromic luminescent materials, optics

Posted Date: February 25th, 2021

DOI: https://doi.org/10.21203/rs.3.rs-226341/v1

Version of Record: A version of this preprint was published at Nature Communications on July 2nd, 2021.
See the published version at https://doi.org/10.1038/s41467-021-24381-5.

Molecular insertion regulates the donor-acceptor interactions in cocrystals for the design of piezochromic luminescent materials

Chunguang Zhai[1], Xiu Yin[1], Shifeng Niu[1], Mingguang Yao[*,1], Shuhe Hu[1], Jiajun Dong[1], Yuchen Shang[1], Zhigang Wang[2], Quanjun Li[1], Bertil Sundqvist[1,3] & Bingbing Liu[*,1]

[1] State Key Laboratory of Superhard Materials, College of Physics, Jilin University, Changchun 130012, China

[2] Institute of Atomic and Molecular Physics, Jilin University, Changchun 130012, China

[3] Department of Physics, Umeå University, SE-90187 Umeå, Sweden

*email: yaomg@jlu.edu.cn; liubb@jlu.edu.cn

Abstract

Developing a universal strategy to design new piezochromic luminescent materials with desirable properties remains challenging. Here, we report that insertion of a non-emissive molecule into a donor (perylene) and acceptor (TCNB) binary cocrystal can realize fine manipulation of intermolecular interactions between perylene and TCNB for desirable piezochromic luminescent properties. A continuous pressure-induced emission enhancement up to 3 GPa and a blue shift from 655 nm to 619 nm have been observed in perylene-TCNB cocrystals upon THF insertion, in contrast to the red-shifted and quenched emission observed when compressing perylene-TCNB cocrystals and other

cocrystals reported earlier. By combining experiment with theory, it is further revealed that the inserted non-emissive THF forms blue-shifted H-bonds with neighboring TCNB molecules and promote a conformation change of perylene molecules upon compression, causing the blue-shifted and enhanced emission. This strategy remains valid when inserting other molecules as non-emissive component into perylene-TCNB cocrystals for abnormal piezochromic luminescent behaviors. Our strategy could also be extended to other cocrystals with different donor-acceptor components, opening a new way for designing novel piezochromic luminescent materials for future applications.

Introduction

Luminescent materials that exhibit remarkable changes in emission color and intensity upon external mechanical stimuli, such as pressing, grinding/shearing and stretching, have been attracting great interest because of their potential for applications in pressure sensors, optical data storage and optoelectronic devices, etc[1–10]. Among these mechanical stimuli, hydrostatic compression is advantageous for a wide range of emission tuning and to build structure-property relationships of materials in a more controllable way[10–14]. So far, most luminescent materials show a gradual red-shifted and quenched emission as pressure increases, which have been explained by different mechanisms, such as exciton coupling[12], orbital overlap[13] and π–π aggregation[15], etc. In contrast, pressure-induced

blue-shifted emission and emission enhancement have only been observed very rarely in luminescent materials upon compression[16]. The design of desirable piezochromic luminescent materials with such anomalous properties for specific applications has long been pursued[9,11]. In particular, π-conjugated organic materials, which include a large family of luminescent materials, have been intensively explored[2,5,6]. Very recently, a man-made crystal consisting of the complicated single-component molecule 9-(4-(1,2,2-triphenylvinyl)phenyl)anthracene was found to exhibit novel piezochromic luminescent behavior upon compression[17]. In this case, a discontinuous piezochromic luminescence was observed. First, normal red-shifted and quenched emission was observed at initial compression (up to 1.23 GPa), and then a new photoluminescence (PL) band with blue-shift and enhanced emission appeared upon further compression to 4.28 GPa. The anomalous luminescent behaviors were explained by a cooperative effect between aggregation-induced emission and energy-transfer suppression.

In contrast to single-component crystals, organic cocrystals (OCCs) are composed of two or more components and the luminescent properties should be more flexible because of their tunable intermolecular interactions and components[18–24]. This provides a large number of candidates for studying piezochromic luminescent behaviors and designing new piezochromic luminescent materials with desirable

properties. Despite recent efforts, the OCCs reported so far mainly exhibit red-shifted emission and quenched PL upon compression[15,25,26]. Thus, it is important and urgent to develop an innovative and universal strategy for designing piezochromic luminescent materials with desirable pressure-responsive properties, which however, remains challenging.

Here, we report a novel strategy by inserting an "inert" molecule, tetrahydrofuran, THF, into perylene-1,2,4,5-tetracyanobezene (TCNB) cocrystals (PTCs) for tailoring the donor (perylene) - acceptor (TCNB) interactions and achieve simultaneous pressure-induced blue-shifted and enhanced emission from the cocrystal. In the designed experiment, THF contains saturated sp^3 bonded carbon atoms (no π electron) and an oxygen atom with paired electrons in *p*/*sp*-orbital, which allows the formation of C-H···O bonding but will not bond covalently with perylene or TCNB. With pressure stabilizing and pushing THF into the PTCs, the interactions between the donor and acceptor (D-A) can be efficiently manipulated. This causes anomalous, simultaneous pressure-induced blue-shifted and enhanced emission in the perylene-TCNB based cocrystals. This strategy has also been shown to be efficient for other molecules inserted into perylene-TCNB cocrystals as non-emissive component for anomalous piezochromic luminescence. We also anticipate that it could be extended to other cocrystals with different D-A components, for example those constructed by aromatic molecules and

classical acceptors, such as 7,7,8,8-tetracyanoquinodimethane (TCNQ)[27] and fullerenes[28].

Results and Discussion

Characterization of PTCs with and without THF at ambient conditions. Fig. 1a shows the X-ray diffraction (XRD) patterns of the PTCs and THF-inserted PTCs (PTCs-THF) sealed in two separated glass capillary tubes. Both are in good agreement with the corresponding XRD patterns of our simulated structures. Both the as-prepared PTCs and the PTCs-THF crystallize in a monoclinic structure but with different cell parameters, as summarized in Supplementary Table S1. Their molecular packings in the corresponding crystals are presented in Fig. 1b and Supplementary Figs. S1-S2. In the cocrystals, perylene is a typical polycyclic aromatic hydrocarbon chromophore as the donor (D) component, while TCNB is the acceptor (A). The donor and acceptor molecules are arranged alternately in a similar molecular column (-DADA-), while neighboring molecular columns are connected to each other, forming a tightly packed stack[11]. For the PTCs, it can be seen that the molecular centers of TCNB and perylene are not above each other, but show a 35% deviation from the accumulation axis[29]; for the PTCs-THF, their center goes back to the same vertical plane. Note that the intercalation of THF molecules would force TCNB to stack toward the edge of perylene. The π-π overlap between one TCNB molecule and

the adjacent perylene molecules is about 50% of a perylene plane[30].

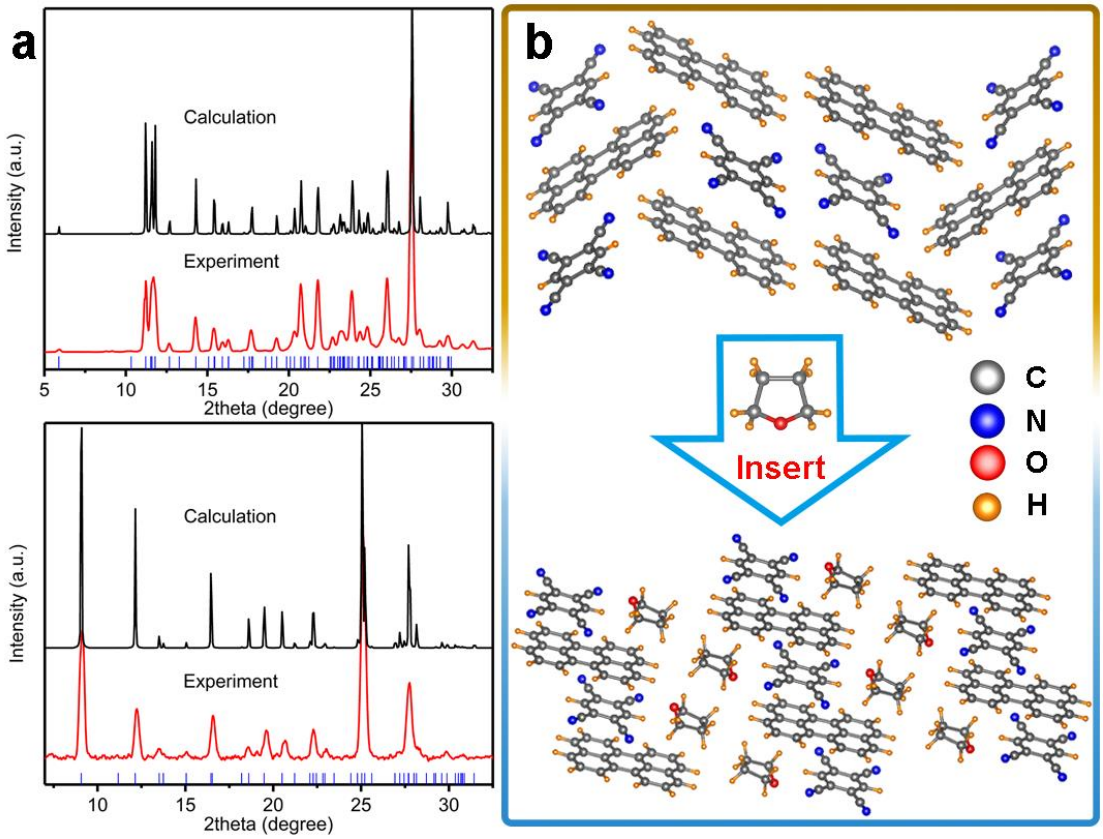

Fig. 1 XRD patterns and crystal packing of PTCs and PTCs-THF. a Experimental and calculated XRD patterns of PTCs (top) and PTCs-THF (bottom). **b** Molecular conformation and crystal packing of PTCs (top) and PTCs-THF (bottom) at ambient conditions.

Piezochromic luminescent properties of PTCs and PTCs-THF. PL spectra of PTCs upon compression up to 5.68 GPa are shown in Fig. 2a. As we can see from the figure, the PL emission of PTCs shows a normal red shift from 720 to 776 nm as pressure increase, accompanied with an obvious decrease in PL intensity. Such pressure-induced emission changes and fluorescence quenching at certain pressures have also been observed in compression experiments on other cocrystals[15,26].

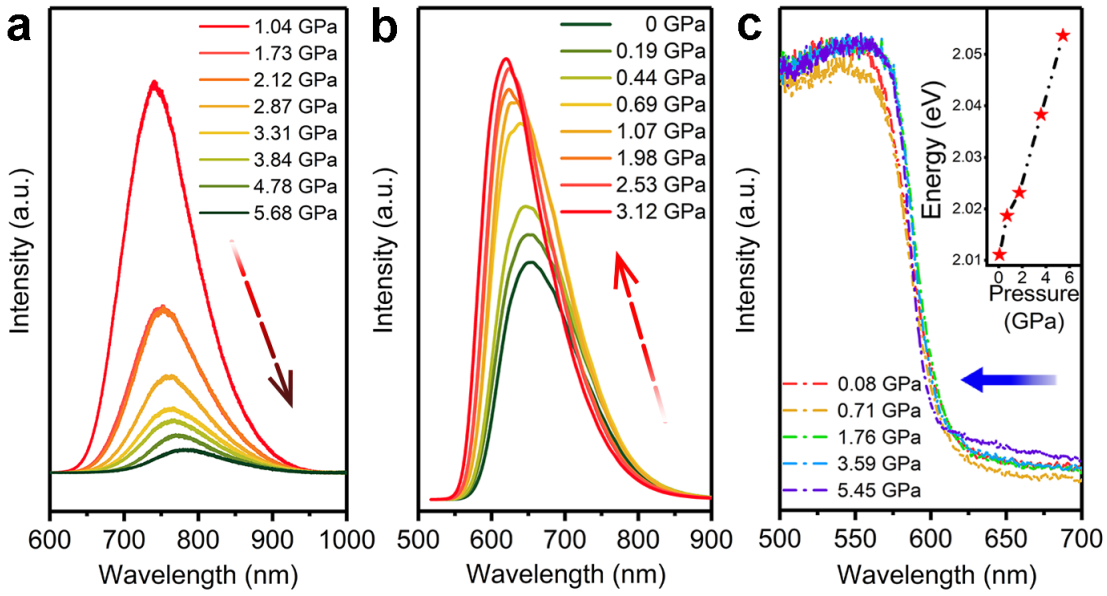

Fig. 2 PL and absorption spectra. a PL spectra of PTCs upon compression up to 5.68 GPa. **b** PL spectra of PTCs-THF up to 3.12 GPa. **c** *In situ* UV-Vis absorption spectra of PTCs-THF up to 5.45 GPa. Inset shows the corresponding pressure dependence of band gap.

To tune the intermolecular interactions between donor and acceptor, THF has been inserted into the lattice of the PTCs to study its effect on the PL emission of the cocrystals. For this, PTCs were soaked in liquid THF in a diamond anvil cell where the greyish-green cocrystals quickly turned red, suggesting that THF molecules penetrated into PTCs, forming PTCs-THF. In this case, THF can be stabilized in the cocrystal by applying pressure and also acts as pressure transmission medium surrounding the sample. Remarkably, PTCs-THF exhibits an abnormal PL behavior as pressure increases. As shown in Fig. 2b, the PL emission bands show a clear blue shift from 655 to 619 nm as pressure increases up to 3.12 GPa, accompanied with a significant enhancement of PL intensity.

At higher pressure above 3.12 GPa, the PL intensity starts to decrease gradually, but the PL emission bands still keep blue-shifting as pressure increases. Supplementary Fig. S3 demonstrates the piezochromic PL spectra of these two cocrystals up to 20 GPa. To study how the band gap of PTCs-THF changes under pressure, *in situ* UV-Vis absorption spectra of the material were measured during compression (Fig. 2c). The absorption edge of PTCs-THF is located at 616.6 nm at 0.08 GPa (the corresponding band gap is 2.01 eV), and exhibits an obvious blue shift during compression. As pressure increases up to 5.45 GPa, the absorption edge of the cocrystal moves to 603.9 nm (corresponding to band gap 2.06 eV) (insert, Fig. 2c). The band gap of the cocrystal thus increases due to the THF insertion, causing the anomalous emission blue-shift as pressure increases. Note that the absorption edge of the cocrystal becomes less sharp and gradually broadens as pressure increases at above 5.45 GPa (Supplementary Fig. S3c), which makes it challenging to derive an accurate band gap of the compressed cocrystal by curve fitting. This also indicates that interactions in the cocrystal become stronger[31].

Structural evolution of PTCs with THF insertion upon compression. To give a further understanding of the effect of THF insertion on the novel PL emission of our cocrystals upon compression, a high-pressure XRD experiment on PTCs-THF has been performed and the recorded XRD patterns are shown in Fig. 3a. All the diffraction peaks shifted to

lower d-values, indicating compression of the lattice. We also present the variation of the unit cell volume with pressure in Fig. 3b. The results suggest that no structural transition happened to PTCs-THF during compression. Instead, the *a-, b-* and *c*-axes exhibit different pressure evolutions upon compression, indicating an anisotropic compression of the lattice (insert, Fig. 3b). Note that above 3 GPa, the *c*-axis was more compressible than the *a*-axis and *b*-axis, indicating that the molecules become more parallel and more closely packed in the *ab* plane (Fig. 3c), which could increase the π-π interactions. Therefore, beyond 3.12 GPa, the reduced distance between D and A in the cocrystal promotes effective π-π stacking interactions that should be responsible for the emission quenching[32].

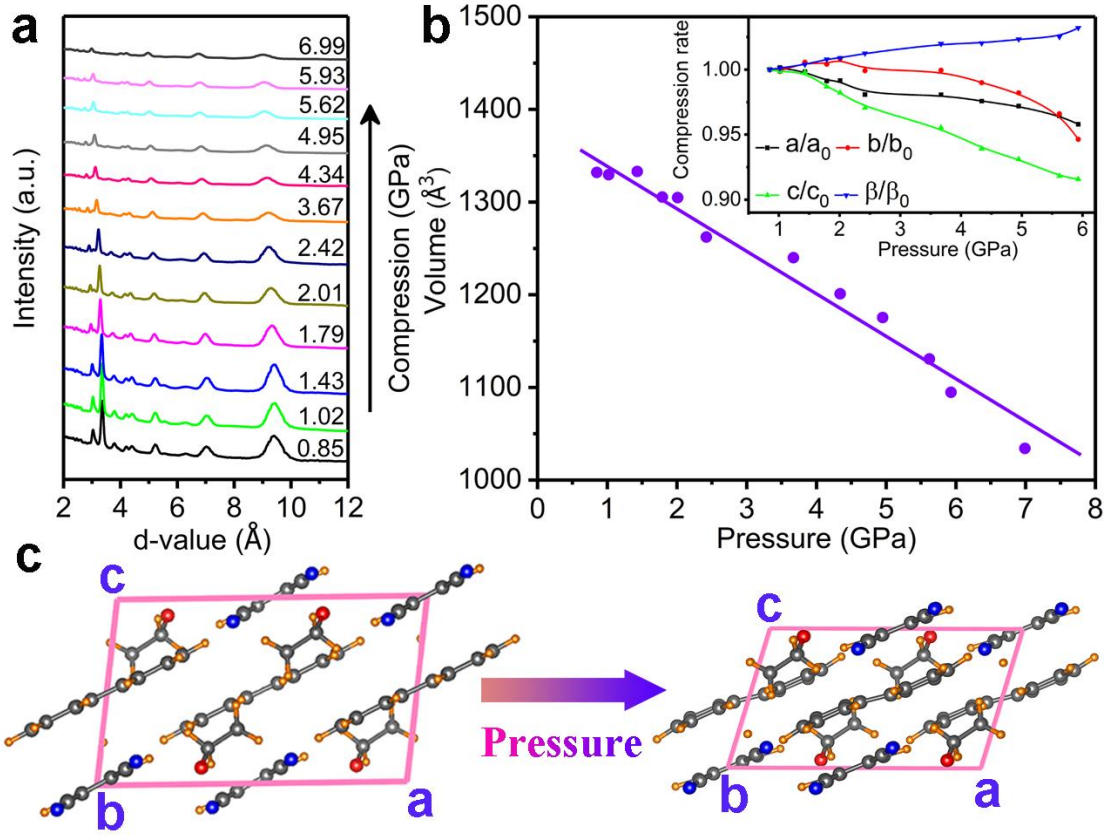

Fig. 3 High-pressure XRD patterns of PTCs-THF. a High-pressure XRD patterns of PTCs-THF up to 6.99 GPa. **b** The plotted curves for the unit cell volume of PTCs-THF as a function of pressure. Inset shows the compression rate of lattice constants as pressure increases. The XRD patterns are analyzed by JADE. **c** Evolution of the molecular arrangement with increasing pressure (view along the b-axis).

Intermolecular interactions of PTCs with THF insertion by IR and Raman spectroscopies. As no structural transition occurred in the compressed cocrystal, the novel PL emission of PTCs-THF should be related to the changes of intermolecular interactions in the cocrystals upon compression. These interactions were studied by Infrared (IR) spectroscopy. As shown in Fig. 4a, the IR spectra of PTCs, THF and

PTCs-THF were measured. Each of their vibrational modes could be assigned according to our theoretically calculated IR spectra (Supplementary Fig. S4). The spectroscopic features from both perylene and TCNB can be clearly distinguished, suggesting only weak van der Waals interactions between the molecules[33]. Upon compression, the IR peaks of PTCs were gradually blue-shifted and broadening (Fig. 4b), showing a common pressure evolution as observed in other molecular crystals[25,34,35]. In contrast, PTCs-THF show obvious differences in the IR spectra (Fig. 4c) compared with those of PTCs under pressure, due to the insertion of THF molecules into the lattice. The insertion of THF clearly results in the formation of H-bonding between THF and TCNB. The C-O-C symmetrical stretching vibration s(C-O-C) from THF, located at 895 cm^{-1}, exhibited a clear red shift as pressure increased, indicating a strengthening of C-H···O hydrogen bonds. As for TCNB, the formation of C-H···O hydrogen bonds also leads to a much higher blue-shift rate of the C-H stretching vibrations ν(C−H) at 3028 and 3108 cm^{-1} in the PTCs-THF than for that in the PTCs upon compression. A similar effect of the H-bond formation on the blue shift of the C-H stretching mode has also been observed in polyglycine II[36]. In addition, the IR peaks at 914 and 1246 cm^{-1} (a new peak appearing at 1.13 GPa), which can be assigned to C-H wagging vibrations ω(C-H) and C-H bending vibrations β(C-H) in TCNB[37], exhibit an obvious enhancement in intensity (Supplementary

Fig. S5), indicating that the polarity of the C-H bond of TCNB increases. This further supports the formation of a blue-shifted H-bond. Consequently, the H-bonding stabilized the TCNB[38–41]. On the other hand, the insertion of THF causes a distortion of the perylene molecule. This is evidenced by the gradual asymmetrization and split of the initially asymmetrical deformation vibrations δas(C-C_{ring}) of perylene (peak at 1586 cm^{-1}) during compression[42] (Supplementary Fig. S6). The distortion of perylene should reduce the π-conjugation[43,44].

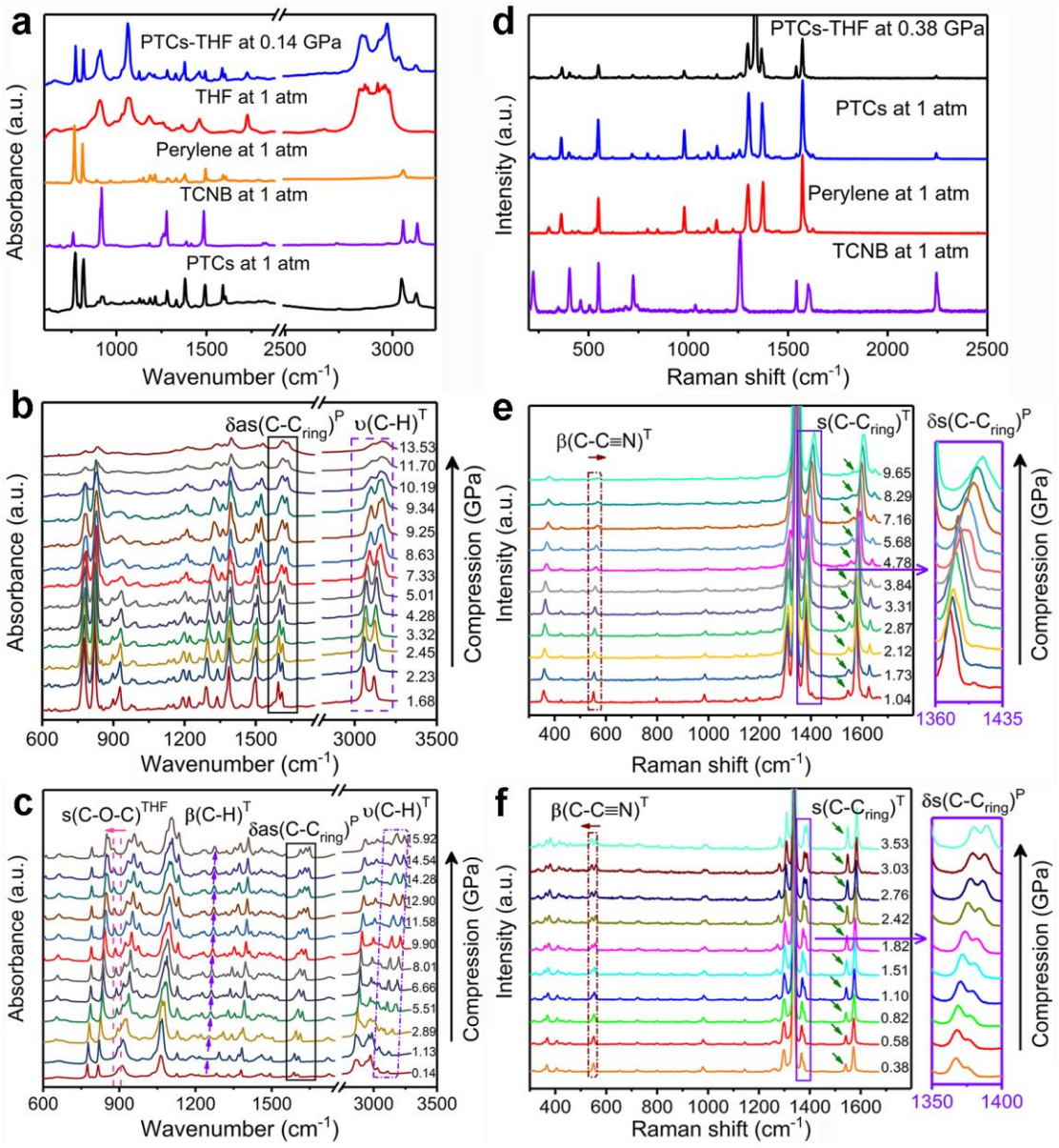

Fig. 4 IR and Raman spectra of PTCs and PTCs-THF. a The IR spectra of PTCs, THF and PTCs-THF at/near ambient conditions. High-pressure IR spectra of **b** PTCs and **c** PTCs-THF. **d** Raman spectra of PTCs, TCNB, Perylene and PTCs-THF at/near ambient conditions. High-pressure Raman spectra of the **e** PTCs and **f** PTCs-THF. The relevant vibrations are marked in the diagram, the different marks in the upper right corner represent the vibration attribution; Marks T and P represent TCNB and perylene, respectively.

Our Raman measurements give further support for the formation of H-bonding when THF is inserted into the cocrystal upon compression. The recorded Raman spectra at ambient and high pressures are shown in Fig. 4e and Fig. 4f. Each vibrational mode of PTCs and PTCs-THF can be assigned, as shown in Fig. 4d and Supplementary Fig. S7. The dependence of peak positions and intensities on pressure for some selected Raman modes is shown in Supplementary Fig. S8. It is clear that the relative peak intensity of the carbon ring stretching vibration $\nu(C\text{-}C_{ring})$ at 1541 cm^{-1} becomes stronger as pressure increases from ambient to 3.53 GPa[37] (Supplementary Fig. S8a), indicating that the polarizability of the C-H bond of TCNB increases[39–41]. This should be related to the enhancement of hydrogen bonding. The Raman peak at 1367 cm^{-1} from symmetrical deformation vibrations $\delta s(C\text{-}C_{ring})$ of perylene gradually splits during compression[42] (Supplementary Fig. S9), which indicates the deformation of perylene, in agreement with our IR results. In addition, the peak located at 549 cm^{-1} from C-C≡N out-plane bending vibration β(C-C≡N) of TCNB exhibits a split at 1.1 GPa and one of the split peaks (545 cm^{-1}) downshifts to low frequency up to 3.03 GPa[37] (Supplementary Fig. S8b), which indicates that THF restricts the C-C≡N out-of-plane bending vibration (Supplementary Fig. S9). This could inhibit non-radiative emission and thus promote PL enhancement.

Besides its capability to form H-bonding with TCNB and affect the

molecular vibrations, as well as to distort the perylene conformation, the THF inserted into the cocrystal also acts as spacer to separate and stabilize the TCNB and perylene molecules due to its “inert” properties (the inability to form covalent bonds). Neither Raman nor IR measurements show any obvious weakening or broadening of any IR or Raman peak from TCNB or perylene upon compression, in contrast to the common pressure evolution of weakening and broadening of the corresponding modes in PTCs upon compression.

Calculation of the molecular orbitals (MO) and photoluminescent properties. The MO were further calculated to analyze the change of the HOMO-LUMO energy gap[15,19] (Fig. 5a). Upon THF insertion, the energy gap is increased from 1.836 eV in PTCs to 2.093 eV in PTCs-THF at ambient pressure (Supplementary Fig. S10). The HOMO is distributed mainly on perylene, while the LUMO is distributed mainly on TCNB. Note that THF is not involved in the observed frontier orbitals distribution. The distribution of frontier orbitals in the cocrystal does not change obviously, but the energy gap of PTCs-THF increases from 2.093 eV to 2.654 eV upon compression from 0 to 20 GPa. Meanwhile, the vertical energy from our calculation also exhibits a similar pressure evolution as the HOMO-LUMO energy gap and becomes larger as pressure increases (Fig. 5b), which agrees well with the experimentally observed blue-shifted emission. The oscillator strengths of the $S_1 \rightarrow S_0$

electronic transition were calculated to analyze the change of the PL intensity[45]. The oscillator strength of PTCs-THF is increased from 0.025 to 0.0362 when pressure is increased from 0 to 5 GPa, while it decreases as pressure increases at above 5 GPa (Fig. 5c). These changes in the oscillator strength, suggesting an increase in emission intensity as pressure increases up to 5 GPa and a gradual quenching above 5 GPa, are in very good agreement with our experiments.

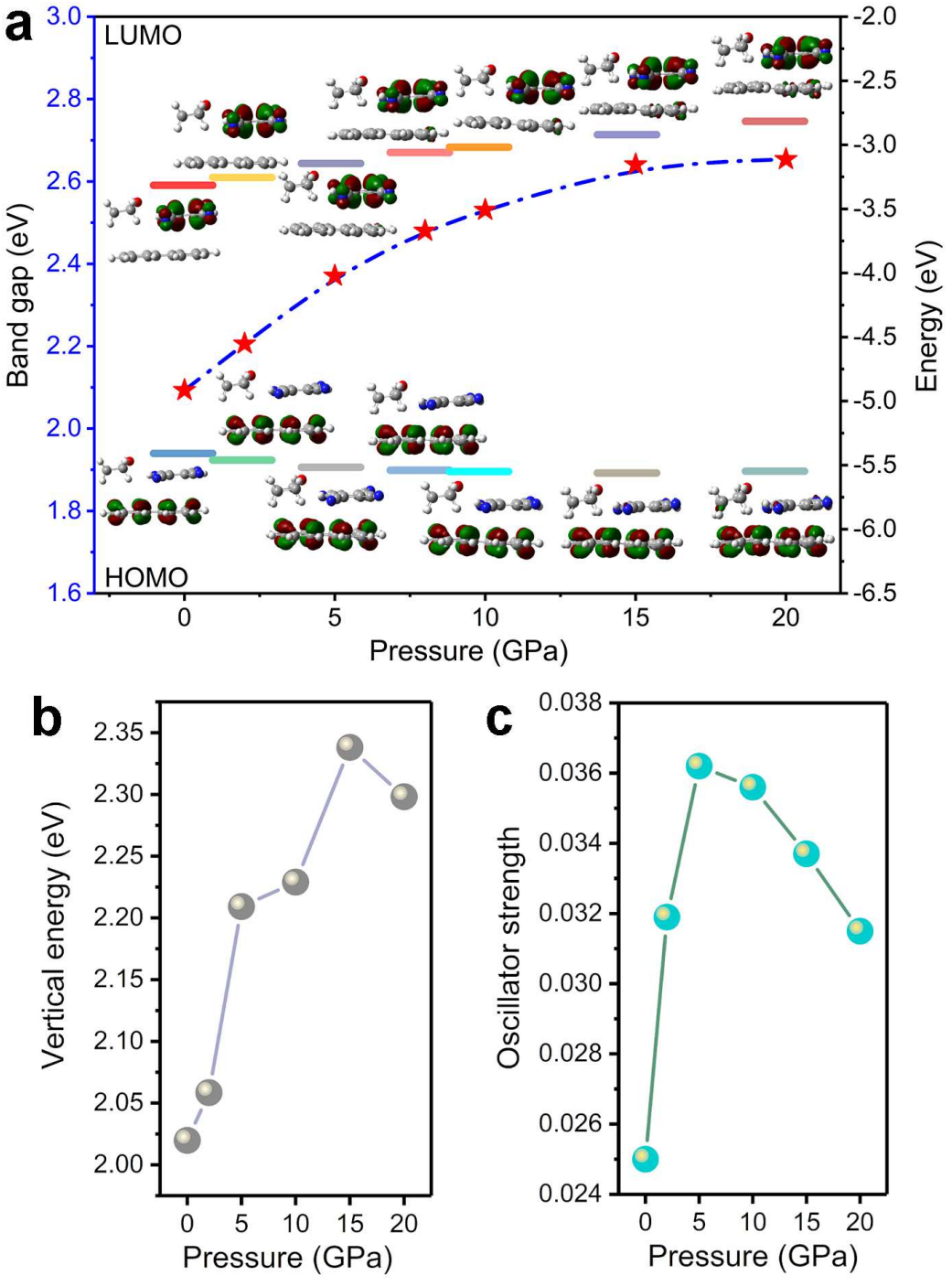

Fig. 5 Calculated MO and optical properties. **a** Calculated HOMO-LUMO energy gap (denoted by red star) of PTC-THF from 0 to 20 GPa. Inset shows the distribution of the frontier orbitals at different pressures. The calculated **b** vertical energy and **c** oscillator strength of PTCs-THF from 0 to 20 GPa.

Analysis of noncovalent interactions (NCI) and molecular configurations. The experimentally observed changes in NCI in the PTCs-THF system have been further studied by the Multiwfn software[46]. As shown in Fig. 6a, the hydrogen bond strength C-H···O increases gradually (colour change from dark green to cyan) as pressure increases[47] (red circles in Fig. 6a). Besides this, the THF insertion also plays a role for isolation and stabilization of TCNB (blue and red circles in Fig. 6a) in the cocrystal upon compression. Moreover, we find that, due to the rigidity of THF molecules, the THF insertion also causes a configurational distortion of the perylene upon compression (see Fig. 6b, the planar perylene turns to a configuration with twisted angle of 7.705 ° at 20 GPa). All our theoretical calculations and experiments thus show that the THF insertion significantly affects the molecular configuration of the donor and the acceptor and their intermolecular interactions, and is thus the main reason for the anomalous pressure-induced blue shift and emission enhancement by affecting the HOMO-LUMO energy gap.

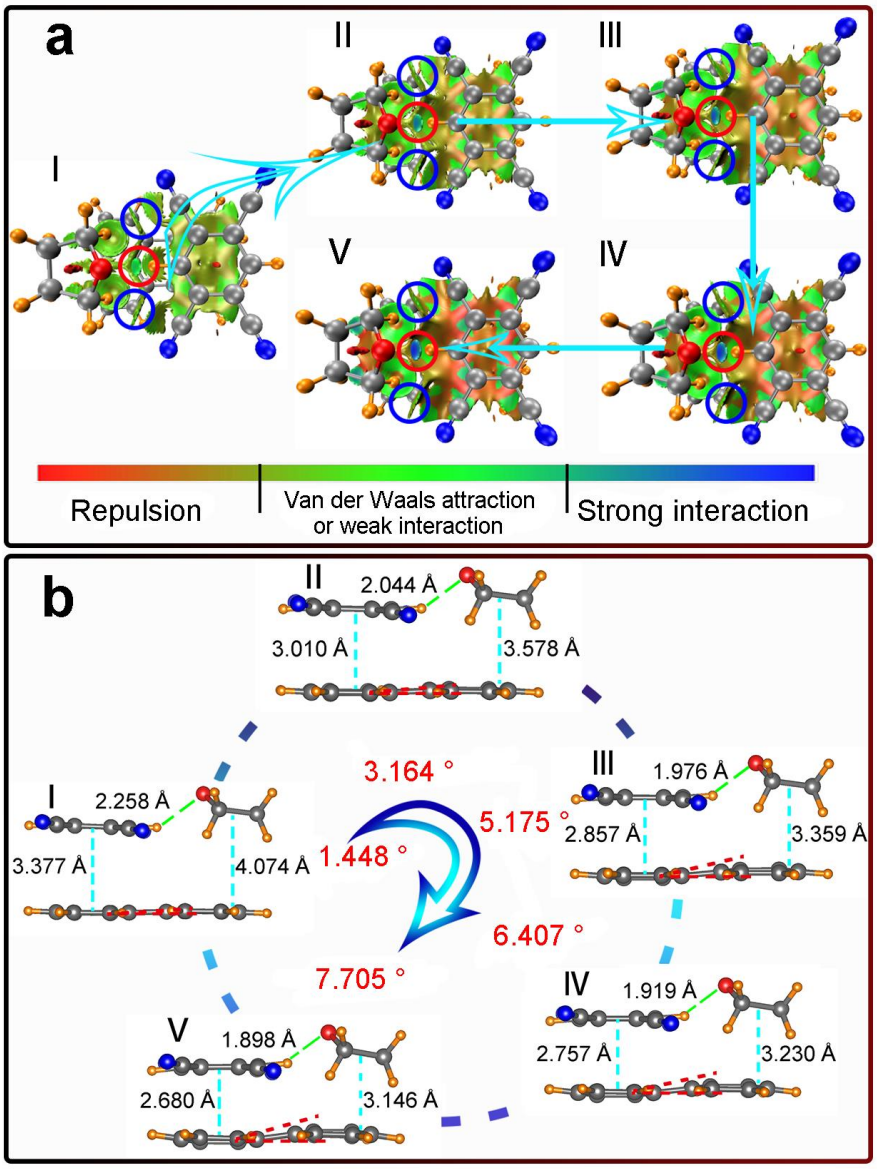

Fig. 6 NCI and molecular configurations analysis. a NCI analysis of PTC-THF at different pressures. The hydrogen bond strength of C-H···O is highlighted by red circles, while the blue circles indicate that Van der Waals forces still exist between TCNB and THF. **b** The molecular configurations at different pressures. The angle (red number) represents the degree of distortion of perylene from 0 to 20 GPa. Roman numerals represent the calculated structure at 0 GPa (I), 5 GPa (II), 10 GPa (III), 15 GPa (IV) and 20 GPa (V).

Discussion

Our results show that molecular insertion can modify and control the interactions between donor and acceptor in a cocrystal. To examine if this strategy is universal for constructing new piezochromic luminescent materials, some other molecules, such as 1,4-dioxane, pyridine, m-xylene, CCl_4, benzene and toluene have also been studied. We found that those molecules analogous to THF, such as 1,4-dioxane and pyridine, are also efficient for achieving photoluminescent materials with anomalous pressure-responsive emission. In these cases, TCNB and perylene act as donor and acceptor, respectively, while the inserted molecule acts as non-emissive component. Note that pressure-induced blue shift and emission enhancement of fluorescence have been observed in these cocrystals, while their enhancement magnitude, pressure-tuned emission range, as well as transition pressures for emission quenching depend on the inserted molecules. In contrast, CCl_4 and m-xylene cannot be inserted into PTCs (Supplementary Fig. S11). The results suggest that our strategy can be extended to other molecules for various piezochromic luminescent behaviors based on perylene-TCNB cocrystals. It is also reasonable to expect that our strategy could be applied to other cocrystals with different donor and acceptor molecules, opening a new way for designing piezochromic luminescent materials. Moreover, it is possible to finely

manipulate certain intermolecular interactions between donor and acceptor in a cocrystal by selecting the inserted non-emissive molecule with specialized functions (such as to form H-bonding and promote molecular deformation by THF). This should also contribute to the design of new materials with desirable properties.

In summary, a new strategy has been demonstrated to achieve novel piezochromic luminescent materials based on perylene-TCNB binary cocrystals by molecular insertion. We show that the insertion of THF, a non-emissive molecule, into perylene-TCNB cocrystal can manipulate intermolecular interactions between donor (perylene) and acceptor (TCNB) for to produce desirable piezochromic luminescent properties. THF can selectively modify certain intermolecular interactions by forming H-bonding with the acceptor and promoting molecular deformation of the donor. This leads to anomalous, simultaneous pressure-induced blue-shift and enhanced emission in the perylene-TCNB based cocrystals, very different from the red-shift and quenched emission in compressing perylene-TCNB cocrystals and other cocrystals reported. This strategy is efficient for other molecules acting as non-emissive component in perylene-TCNB cocrystals, resulting in anomalous piezochromic luminescent behaviors. We also believe this strategy can be extended to other cocrystals with different donor and acceptor molecules, opening a new way for designing novel external stimuli-responsive PL

materials for future applications.

Methods

Material source. Perylene (98%) and 1,2,4,5-tetracyanobenzene (TCNB, 97%) were purchased from Tokyo Chemical Industry Co., Ltd. (TCI). Tetrahydrofuran (THF, HPLC) was purchased from Sinopharm Chemical Reagent Co., Ltd. All of the chemicals were used as received without further purification.

Material synthesis and crystal structure. The PTCs were obtained by a solvent evaporation method, which has been reported elsewhere[11,15,21,27,30]. In brief, equimolar quantities of perylene (25.2 mg) and TCNB (17.8 mg) were dispersed in 20 mL THF with ultrasonication, and an orange yellow solution was obtained. The blackish green PTCs were obtained after evaporation of solvent from the solution at ambient conditions[30]. The as-synthesized PTCs had the same structure as those grown from CH_2Cl_2[29] (Cambridge Crystallographic Data Centre (CCDC) number, 1248027). The PTCs-THF were obtained by immersing PTCs in THF solvent sealed in a capillary tube or diamond anvil cell and had the same structure as that reported in Ref. 30 (CCDC number, 1847279), but with different cell parameters according to our structural optimization of the experiment by using VASP code. The X-ray diffraction patterns of PTCs and PTCs-THF were calculated by using Materials Studio. DFT calculations were performed to determine the crystal structures at

different pressures.

Experimental details. High-pressure experiments were performed in a diamond anvil cell (DAC). Samples were loaded into a 120 μm diameter hole drilled in the T301 stainless steel gasket. Pressure was calibrated by the fluorescence emission of ruby in the sample chamber. PL measurements were performed on a Raman spectrometer (Renishaw in Via) in the fluorescence mode with a 514.5 nm laser excitation. UV-Visible absorption spectra were collected using a home-built fluorescence microscope equipped with a Horiba Jobin Yvon iHR320 spectrometer. Raman measurements were performed using the spectrometer (Renishaw in Via) equipped with 514.5 nm and 830 nm lasers. Infrared measurements were carried out using a Bruker spectrometer. *In situ* high-pressure X-ray diffraction experiments were performed at the Rigaku Synergy Custom FR-X (λ = 0.7093 Å). Ambient pressure X-ray diffraction experiments were performed at the Rigaku MicroMax-007HFat (λ =1.5418 Å).

Computational details. Our calculations were performed using first-principles plane-wave pseudopotential density functional theory (DFT) as implemented in the VASP code[48]. The projected augmented wave (PAW) method was employed with the PAW potentials taken from the VASP library where $2s^2\ 2p^2$, $2s^2\ 2p^3$ and $2s^2\ 2p^4$ were treated as the valence electrons of C, N and O atoms, respectively. A cutoff energy of

520 eV and an appropriate Monkhorst-Pack k-mesh density of 2π×0.03 $Å^{-1}$ are chosen to ensure that the enthalpy calculations are well converged to less than 1 meV/atom. The generalized gradient approximation (GGA) Perdew-Burke-Ernzerhof (PBE) was used to describe the exchange-correlation interactions. The molecular orbitals of complexes were calculated using the B3LYP/6-31G (d, p). We calculated the properties of PTCs-THF in the crystal phase by using the QM/MM method with a two-layer ONIOM approach. The central TCNB-Perylene-THF was selected as high layer and treated by using the QM method, while the surrounding molecules were chosen as the lower layer and simulated by using the MM method. We adopted M06-2X/6-31G (d, p) to study for QM and universal force field (UFF) was applied for MM, the electronic embedding was adopted to describe the coupling of the QM/MM interfaces. All the calculations above were carried out in the Gaussian 09 package[49].

Data availability

Data that support the findings of this study are available from the corresponding author upon reasonable request.

Acknowledgements

This work was supported financially by the National Key R&D Program of China (2018YFA0305900), the National Natural Science Foundation of China (51822204), the Program for JLU Science and

Technology Innovative Research Team (2017TD-01), the Program of China Postdoctoral Science Foundation (2020TQ0121).

Author contributions

M. Y. supervised the research; M. Y., B. L. and C. Z. designed the experiments; C. Z. carried out the materials synthesis, characterization and high-pressure experiments; X. Y., S. N. and Z. W. performed the theoretical calculation; C. Z. and S. H. collected *in situ* UV-Vis absorption spectra and analyzed the data; C. Z. and Q. L. collected *in situ* XRD spectra; C. Z. and J. D. analyzed the IR and Raman data; C. Z. and Y. S. design and drew the figures; M. Y., C. Z., B. L. and B. S. wrote the manuscript and all authors discussed the results and the manuscript.

Competing interests

The authors declare no competing interests.

Reference

1. Davis, D. A. *et al.* Force-induced activation of covalent bonds in mechanoresponsive polymeric materials. *Nature* **459**, 68–72 (2009).
2. Sagara, Y., Yamane, S., Mutai, T., Araki, K. & Kato, T. A stimuli-responsive, photoluminescent, anthracene-based liquid crystal: Emission color determined by thermal and mechanical processes. *Adv. Funct. Mater.* **19**, 1869–1875 (2009).
3. Sagara, Y. & Kato, T. Brightly tricolored mechanochromic luminescence from a single-luminophore liquid crystal: Reversible

writing and erasing of images. *Angew. Chem. Int. Ed.* **50**, 9128–9132 (2011).

4. Sun, H. *et al.* Smart responsive phosphorescent materials for data recording and security protection. *Nat. Commun.* **5**, 3601 (2014).
5. Stuart, M. A. C. *et al.* Emerging applications of stimuli-responsive polymer materials. *Nat. Mater.* **9**, 101–113 (2010).
6. Yoon, S.-J. *et al.* Multistimuli two-color luminescence switching via different slip-stacking of highly fluorescent molecular sheets. *J. Am. Chem. Soc.* **132**, 13675–13683 (2010).
7. Ito, H. *et al.* Reversible mechanochromic luminescence of $[(C_6F_5Au)_2(\mu\text{-}1,4\text{-diisocyanobenzene})]$. *J. Am. Chem. Soc.* **130**, 10044–10045 (2008).
8. Yan, D., Yang, H., Meng, Q., Lin, H. & Wei, M. Two-component molecular materials of 2,5-diphenyloxazole exhibiting tunable ultraviolet/blue polarized emission, pump-enhanced luminescence, and mechanochromic response. *Adv. Funct. Mater.* **24**, 587–594 (2014).
9. Lavrenova, A. *et al.* Mechano- and thermoresponsive photoluminescent supramolecular polymer. *J. Am. Chem. Soc.* **139**, 4302−4305 (2017).
10. Wu, J. *et al.* Molecular engineering of mechanochromic materials by programmed C–H arylation: Making a counterpoint in the chromism

trend. *J. Am. Chem. Soc.* **138**, 12803–12812 (2016).

11. Sun, L., Yang, F., Zhang, X. & Hu, W. Stimuli-responsive behaviors of organic charge transfer cocrystals: Recent advances and perspectives. *Mater. Chem. Front.* **4**, 715–728 (2020).
12. Nagura, K. *et al.* Distinct responses to mechanical grinding and hydrostatic pressure in luminescent chromism of tetrathiazolylthiophene. *J. Am. Chem. Soc.* **135**, 10322–10325 (2013).
13. Dong, Y. *et al.* Piezochromic luminescence based on the molecular aggregation of 9,10-Bis((E)-2-(pyrid-2-yl)vinyl)anthracene. *Angew. Chem. Int. Ed.* **51**, 10782 –10785 (2012).
14. Feng, C. *et al.* Unique piezochromic fluorescence behavior of organic crystal of carbazole-substituted CNDSB. *Chem. Commun.* **52**, 3836–3839 (2016).
15. Wang, J. *et al.* Tunable luminescence of a novel organic co-crystal based on intermolecular charge transfer under pressure. *J. Mater. Chem. C* **6**, 8958–8965 (2018).
16. Ma, Z. *et al.* Pressure-induced emission of cesium lead halide perovskite nanocrystals. *Nat. Commun.* **9**, 4506 (2018).
17. Liu, H. *et al.* Pressure-induced blue-shifted and enhanced emission: A cooperative effect between aggregation-induced emission and energy-transfer suppression. *J. Am. Chem. Soc.* **142**, 1153–1158 (2020).

18. Haketa, Y. *et al.* Oriented salts: Dimension-controlled charge-by-charge assemblies from planar receptor-anion complexes. *Angew. Chem. Int. Ed.* **49**, 10079–10083 (2010).
19. Zhu, W. *et al.* Revealing the charge-transfer interactions in self-assembled organic cocrystals: Two-dimensional photonic applications. *Angew. Chem.* **127**, 6889–6893 (2015).
20. Gong, X., Wang, S., Moses, D., Bazan, G. C. & Heeger, A. J. Multilayer polymer light-emitting diodes: White-light emission with high efficiency. *Adv. Mater.* **17**, 2053–2058 (2005).
21. Zhu, W. *et al.* Rational design of charge-transfer interactions in halogen-bonded co-crystals toward versatile solid-state optoelectronics. *J. Am. Chem. Soc.* **137**, 11038–11046 (2015).
22. Lei, Y. *et al.* Revealing insight into long-lived room-temperature phosphorescence of host–guest systems. *J. Phys. Chem. Lett.* **10**, 6019–6025 (2019).
23. Yan, D., Yang, H., Meng, Q., Lin, H. & Wei, M. Two-component molecular materials of 2,5-diphenyloxazole exhibiting tunable ultraviolet/blue polarized emission, pump-enhanced luminescence, and mechanochromic response. *Adv. Funct. Mater.* **24**, 587–594 (2014).
24. Lei, Y. L., Liao, L. S. & Lee, S. T. Selective growth of dual-color-emitting heterogeneous microdumbbells composed of

organic charge-transfer complexes. *J. Am. Chem. Soc.* **135**, 3744–3747 (2013).

25. Lu, B. *et al.* Piezochromic luminescence of AIE-active molecular co-crystals: Tunable multiple hydrogen bonding and molecular packing. *J. Mater. Chem. C* **6**, 9660–9666 (2018).
26. Liu, Y. *et al.* Piezochromic luminescence of donor–acceptor cocrystals: Distinct responses to anisotropic grinding and isotropic compression. *Angew. Chem. Int. Ed.* **57**, 15670–15674 (2018).
27. Zhu, W., Yi, Y., Zhen, Y. & Hu, W. Precisely tailoring the stoichiometric stacking of perylene-TCNQ co-crystals towards different nano and microstructures with varied optoelectronic performances. *Small* **11**, 2150–2156 (2015).
28. Zhang, J. *et al.* Fullerene/sulfur-bridged annulene cocrystals: Two-dimensional segregated heterojunctions with ambipolar transport properties and photoresponsivity. *J. Am. Chem. Soc.* **135**, 558–561 (2013).
29. Bock, H., Seitz, W., Sievert, M., Kleine, M. & Bats, J. W. Donor/acceptor complexes in hydrogen-bonded networks: PH-dependent self-organization. *Angew. Chem. Int. Ed. Engl.* **35**, 2244–2246 (1996).
30. Sun, Y., Lei, Y., Dong, H., Zhen, Y. & Hu, W. Solvatomechanical bending of organic charge transfer cocrystal. *J. Am. Chem. Soc.* **140**,

6186–6189 (2018).

31. Zhang, S. *et al.* Rehybridization of nitrogen atom induced photoluminescence enhancement under pressure stimulation. *Adv. Funct. Mater.* **27**, 1602276 (2017).

32. Heimel, G. *et al.* Phase transition and electronic properties of fluorene: A joint experimental and theoretical high-pressure study. *Phys. Rev. B* **73**, 024109 (2006).

33. Zhang, Y. *et al.* Negative Volume Compressibility in $Sc_3N@C_{80}$-cubane cocrystal with charge transfer. *J. Am. Chem. Soc.* **142**, 7584–7590 (2020).

34. Cui, W. *et al.* A new carbon phase constructed by long-range ordered carbon clusters from compressing C_{70} solvates. *Adv. Mater.* **26**, 7257–7263 (2014).

35. Yao, M. *et al.* Tailoring building blocks and their boundary interaction for the creation of new, potentially superhard, carbon materials. *Adv. Mater.* **27**, 3962–3968 (2015).

36. Krimm, S. & Kuroiwa, K. Low temperature infrared spectra of polyglycines and C-H···O=C hydrogen bonding in polyglycine II. *BIOPOLYMERS* **6**, 401-407 (1968).

37. Pawlukoj, A. *et al.* The structure, methyl rotation reflected in inelastic and quasielastic neutron scattering and vibrational spectra of 1,2,3,5-tetramethoxybenzene and its 2:1 complex with

1,2,4,5-tetracyanobenzene. *J. Chem. Phys.* **129**, 154506 (2008).

38. Qian, W. & Krimm, S. Vibrational spectroscopy of hydrogen bonding: Origin of the different behavior of the C−H···O hydrogen bond. *J. Phys. Chem. A* **106**, 6628-6636 (2002).

39. van der Veken, B. J. *et al.* The nature of improper, blue-shifting hydrogen bonding verified experimentally. *J. Am. Chem. Soc.* **123**, 12290–12293 (2001).

40. Li, X., Liu, L. & Schlegel, H. B. On the physical origin of blue-shifted hydrogen bonds. *J. Am. Chem. Soc.* **124**, 9639–9647 (2002).

41. Alabugin, I. V., Manoharan, M., Peabody, S. & Weinhold, F. Electronic basis of improper hydrogen bonding: A subtle balance of hyperconjugation and rehybridization. *J. Am. Chem. Soc.* **125**, 5973–5987 (2003).

42. Ong, K. K., Jensen, J. O. & Hameka, H. F. Theoretical studies of the infrared and raman spectra of perylene. *J. Mol. Struct. THEOCHEM* **459**, 131–144 (1999).

43. Cozzi, F., Cinquini, M., Annunziata, R., Dwyer, T. & Siegel, J. S. Polar/π interactions between stacked aryls in 1,8-diarylnaphthalenes. *J. Am. Chem. Soc.* **114**, 5729–5733 (1992).

44. Hoeben, F. J. M., Jonkheijm, P., Meijer, E. W. & Schenning, A. P. H. J. About supramolecular assemblies of π-conjugated systems. *Chem. Rev.* **105**, 1491–1546 (2005).

45. Shi, Y. *et al.* Pressure-induced emission (PIE) of one-dimensional organic tin bromide perovskites. *J. Am. Chem. Soc.* **141**, 6504–6508 (2019).
46. Lu, T. & Chen, F. Multiwfn: A multifunctional wavefunction analyzer. *J. Comput. Chem.* **33**, 580–592 (2012).
47. Johnson, E. R. *et al.* Revealing noncovalent interactions. *J. Am. Chem. Soc.* **132**, 6498–6506 (2010).
48. Kresse, G. & Furthmüller, J. Efficient iterative schemes for *ab initio* total-energy calculations using a plane-wave basis set. *Phys. Rev. B* **54**, 11169–11186 (1996).
49. Frisch, M. J. *et al.* Gaussian 09. (Gaussian, Inc., Wallingford CT, 2009).

Figures

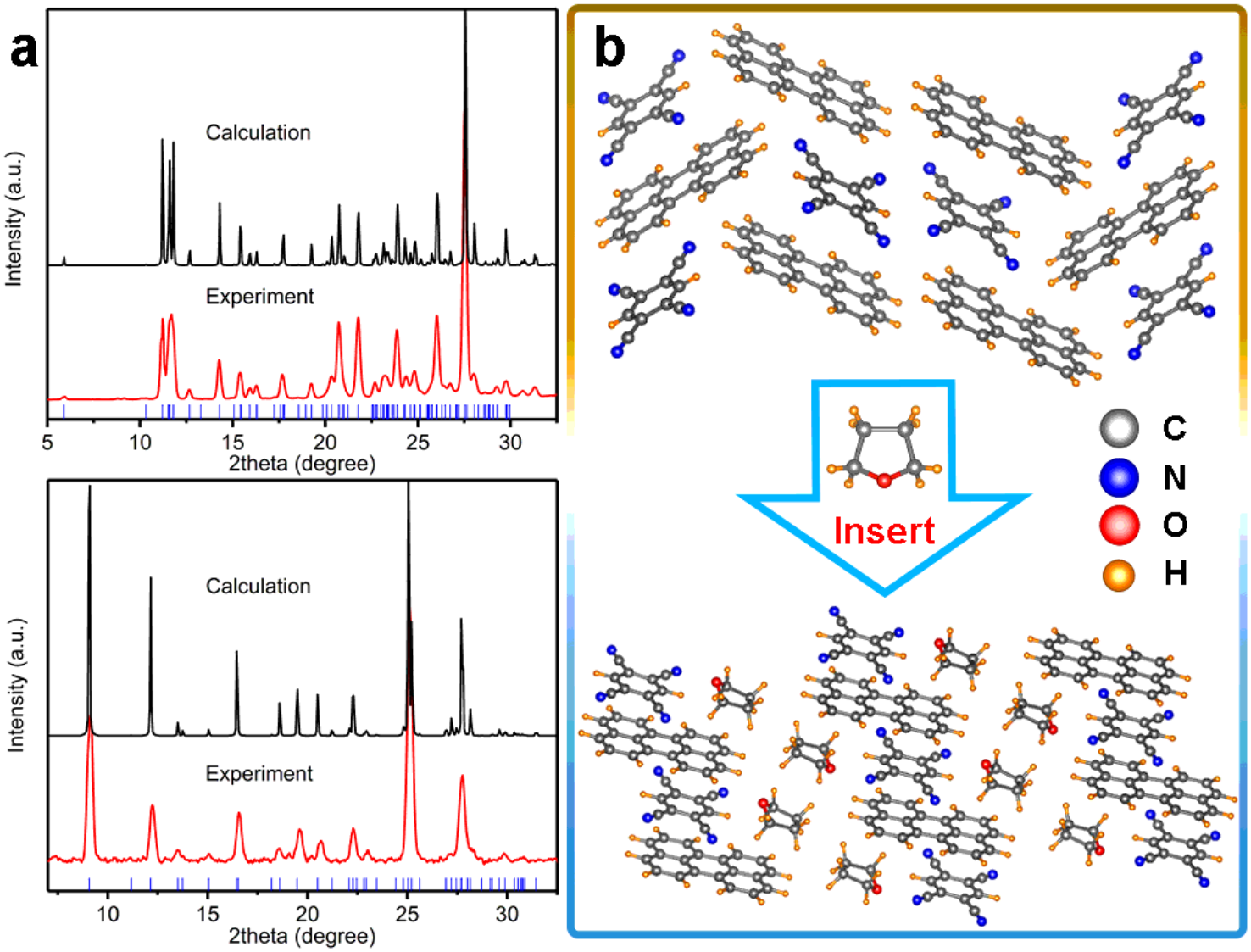

Figure 1

XRD patterns and crystal packing of PTCs and PTCs-THF. a Experimental and calculated XRD patterns of PTCs (top) and PTCs-THF (bottom). b Molecular conformation and crystal packing of PTCs (top) and PTCs-THF (bottom) at ambient conditions.

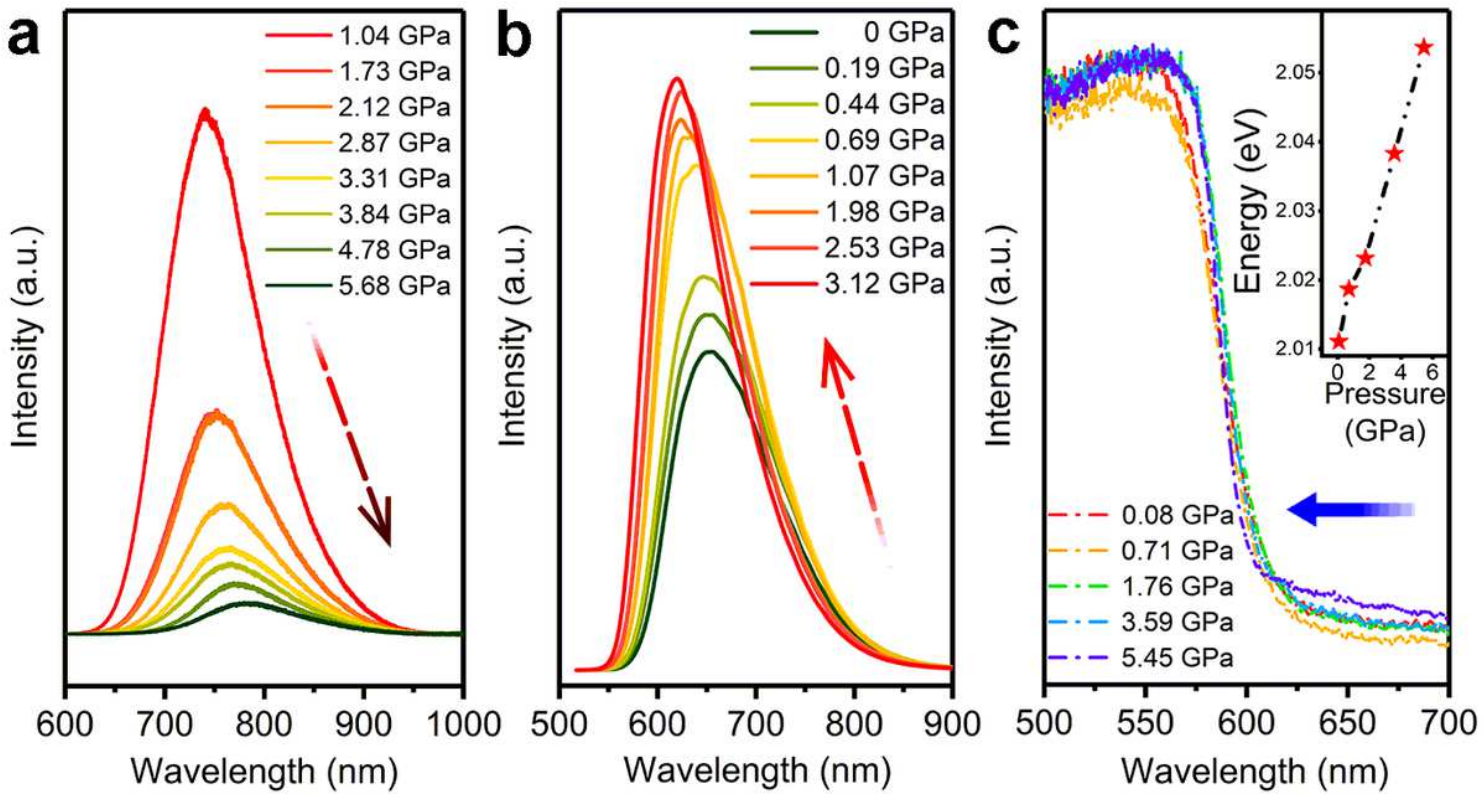

Figure 2

PL and absorption spectra. a PL spectra of PTCs upon compression up to 5.68 GPa. b PL spectra of PTCs-THF up to 3.12 GPa. c In situ UV-Vis absorption spectra of PTCs-THF up to 5.45 GPa. Inset shows the corresponding pressure dependence of band gap.

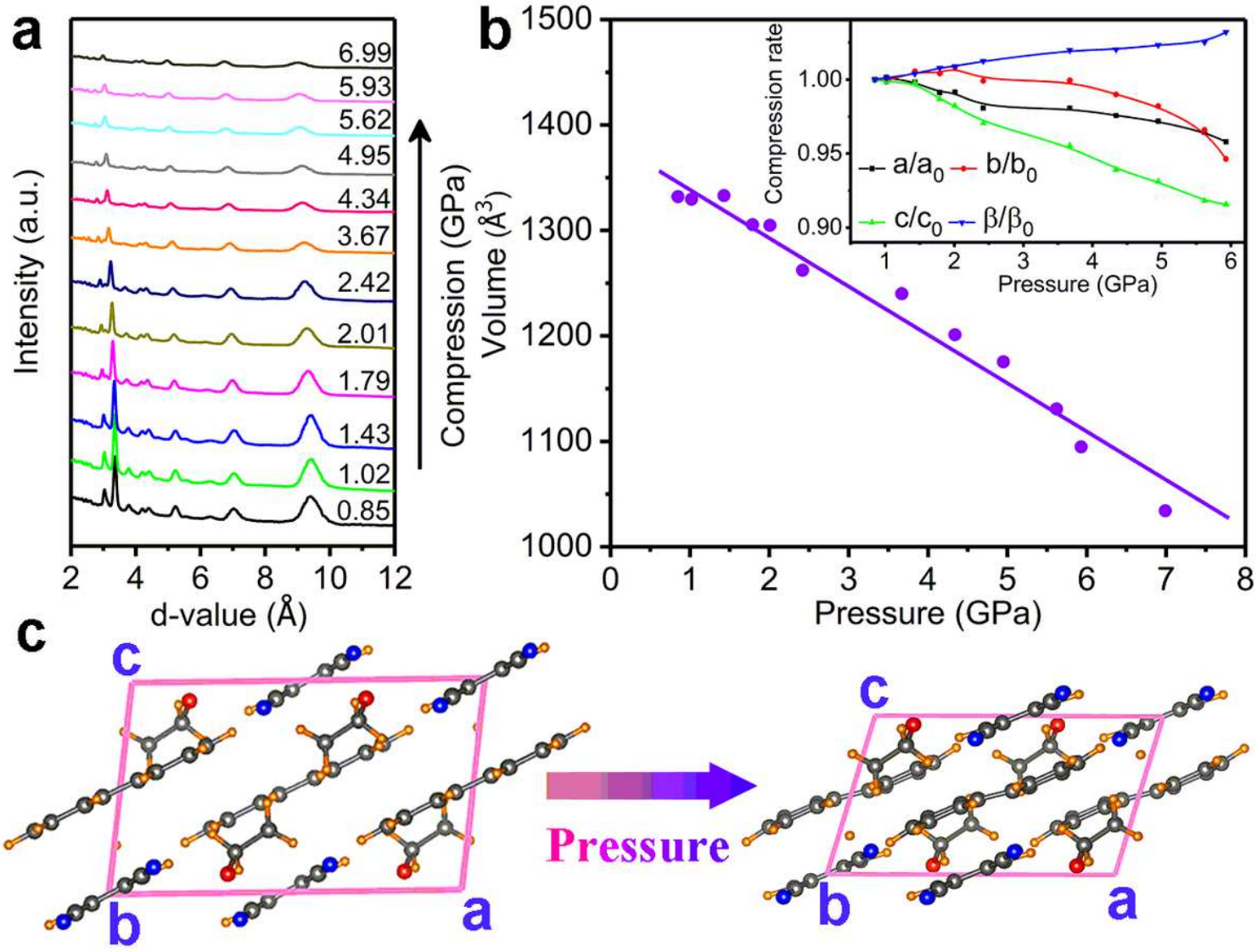

Figure 3

High-pressure XRD patterns of PTCs-THF. a High-pressure XRD patterns of PTCs-THF up to 6.99 GPa. b The plotted curves for the unit cell volume of PTCs-THF as a function of pressure. Inset shows the compression rate of lattice constants as pressure increases. The XRD patterns are analyzed by JADE. c Evolution of the molecular arrangement with increasing pressure (view along the b-axis).

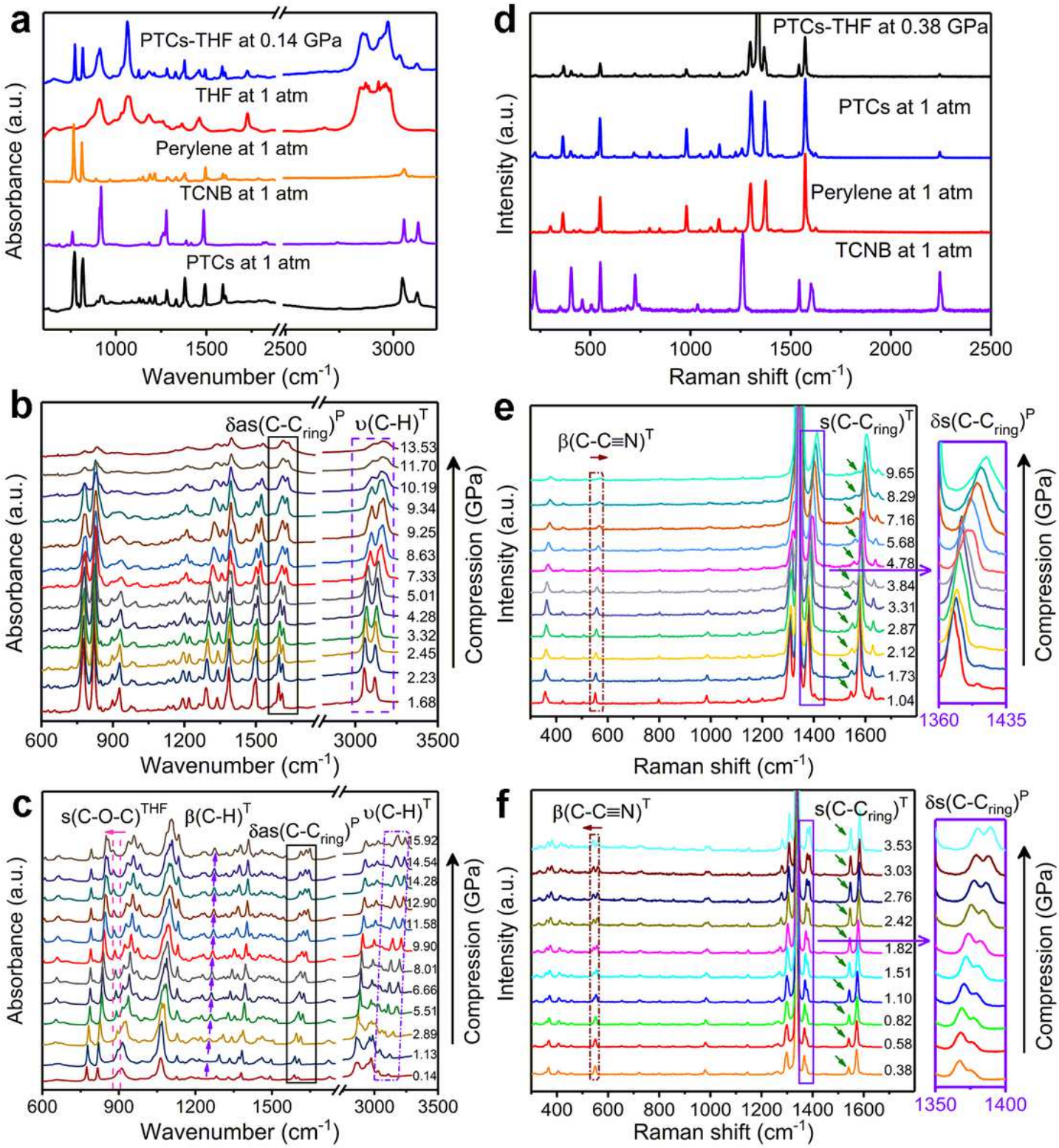

Figure 4

IR and Raman spectra of PTCs and PTCs-THF. a The IR spectra of PTCs, THF and PTCs-THF at/near ambient conditions. High-pressure IR spectra of b PTCs and c PTCs-THF. d Raman spectra of PTCs, TCNB, Perylene and PTCs-THF at/near ambient conditions. High-pressure Raman spectra of the e PTCs and f PTCs-THF. The relevant vibrations are marked in the diagram, the different marks in the upper right corner represent the vibration attribution; Marks T and P represent TCNB and perylene, respectively.

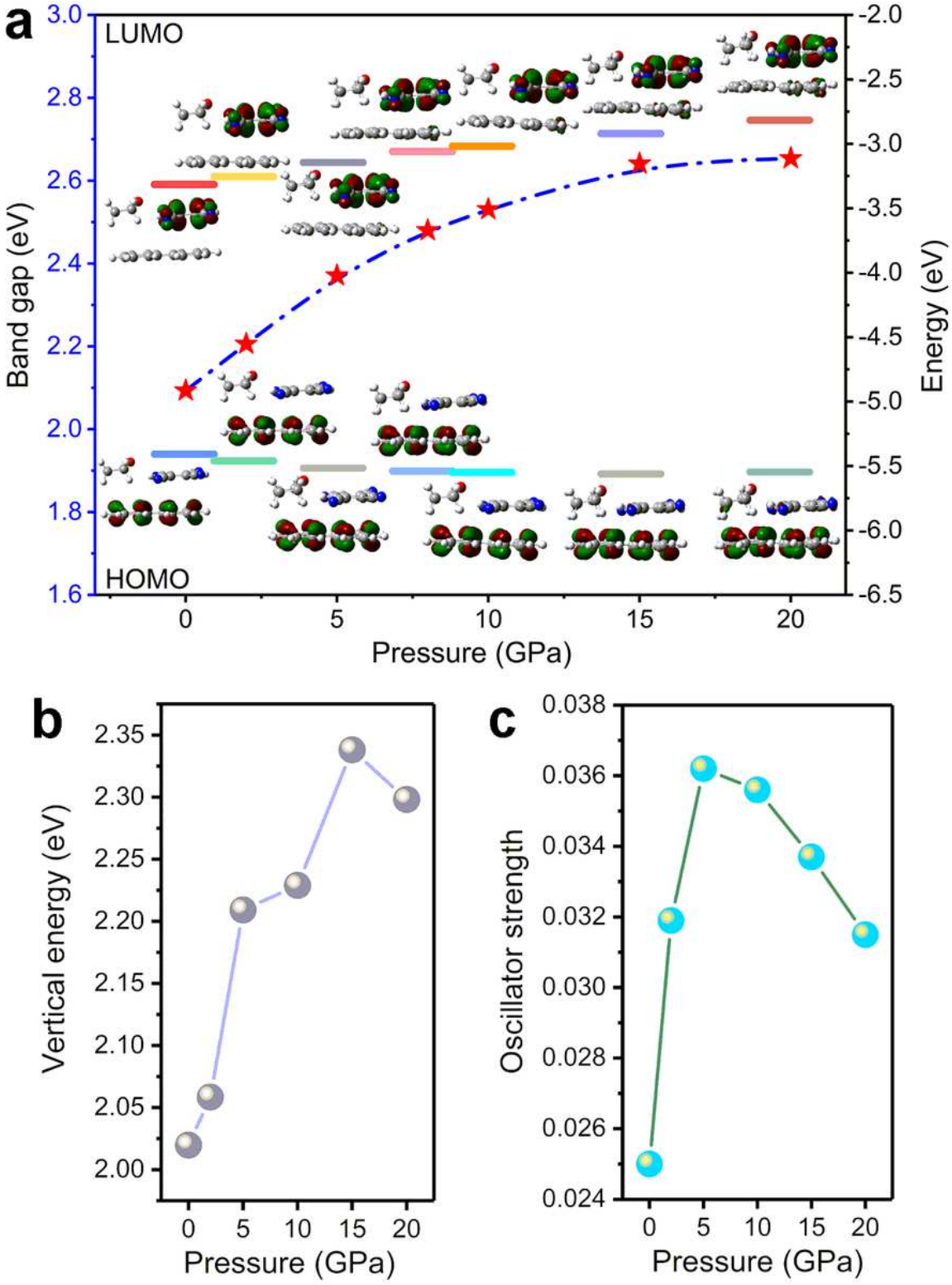

Figure 5

Calculated MO and optical properties. a Calculated HOMO-LUMO energy gap (denoted by red star) of PTC-THF from 0 to 20 GPa. Inset shows the distribution of the frontier orbitals at different pressures. The calculated b vertical energy and c oscillator strength of PTCs-THF from 0 to 20 GPa.

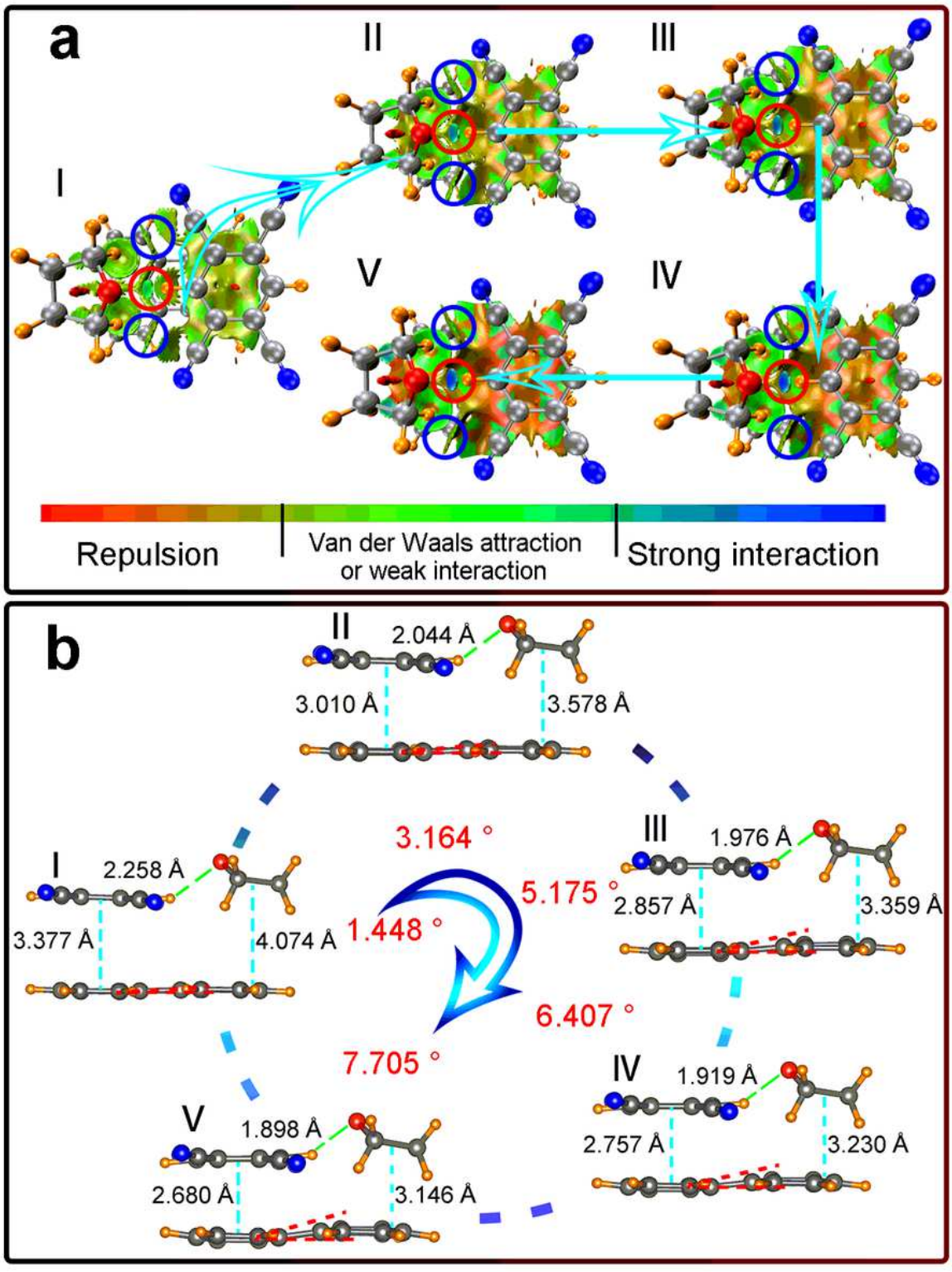

Figure 6

NCI and molecular configurations analysis. a NCI analysis of PTC-THF at different pressures. The hydrogen bond strength of C-H···O is highlighted by red circles, while the blue circles indicate that Van der Waals forces still exist between TCNB and THF. b The molecular configurations at different pressures. The angle (red number) represents the degree of distortion of perylene from 0 to 20 GPa. Roman

numerals represent the calculated structure at 0 GPa (I), 5 GPa (II), 10 GPa (III), 15 GPa (IV) and 20 GPa (V).

Supplementary Files

This is a list of supplementary files associated with this preprint. Click to download.

- SupportingInformation.pdf